THE JOURNAL OF PHYSICAL CHEMISTRY B

Article

pubs.acs.org/JPCB

Photophysics of 3,3′-Diethyloxadicarbocyanine Iodide (DODCI) in Ionic Liquid Micelle and Binary Mixtures of Ionic Liquids: Effect of Confinement and Viscosity on Photoisomerization Rate

Surajit Ghosh, Sarthak Mandal, Chiranjib Banerjee, Vishal Govind Rao, and Nilmoni Sarkar*

Department of Chemistry, Indian Institute of Technology, Kharagpur 721302, WB, India

Supporting Information

ABSTRACT: The dynamics of photoisomerization of 3,3′-diethyloxadicarbocyanine iodide (DODCI) has been investigated inside micellar environment formed by a surfactant-like ionic liquid, 1-butyl-3-methylimidazolium octyl sulfate ($[C_4mim][C_8SO_4]$) and also in binary mixture of another ionic liquid, *N*,*N*,*N*-trimethyl-*N*-propyl ammonium bis(trifluoromethanesulfonyl) imide, ($[N_{3111}][Tf_2N]$) with methanol, acetonitrile, and *n*-propanol by using steady-state and picosecond time-resolved fluorescence spectroscopy. The entrapment of DODCI into the $[C_4mim][C_8SO_4]$ micellar environment led to the enhanced fluorescence intensity along with ∼13 nm red shift in the emission maxima. A sharp increase in the fluorescence quantum yield (Φ) and the lifetime (τ_f) near the critical micelle concentration (cmc) range is observed followed by saturation at higher concentration. As a result of partitioning of the probe molecules in the micellar phase from water, the nonradiative rate constant (k_{nr}) of DODCI decreases 2.7 times than in water. The retardation of isomerization rate is due to high microviscosity of the micellar system compared to bulk water. In order to understand how the rate of isomerization depends on polarity as well as viscosity, we have measured isomerization rate in neat $[N_{3111}][Tf_2N]$ and its mixtures with polar solvents, like methanol, acetonitrile, and *n*-propanol. The addition of methanol and *n*-propanol increases the polarity, but viscosity of the medium decreases. The nonradiative rate constant that represents the rate of photoisomerization decreases with the addition of the polar solvent in $[N_{3111}][Tf_2N]$. Complete analysis of all the experimental results indicate that viscosity is the sole parameter that regulates the rate of photoisomerization. Temperature-dependent k_{nr} are used to determine the activation energy (E_a) in 100 mM $[C_4mim][C_8SO_4]$ solution and neat $[N_{3111}][Tf_2N]$ system.

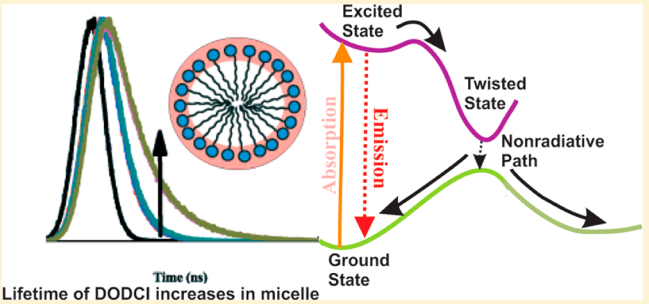

1. INTRODUCTION

Room temperature ionic liquids (RTILs) have generated great interest due to their unique features such as high ionic conductivity, low vapor pressure, favorable solvating properties for a range of polar and nonpolar compounds, and a wide liquidous temperature range.[1−12] RTILs consist of bulky organic cations and inorganic anions, and they are liquid at room temperature and pressure. The properties like hydrophobicity, viscosity, and density can be modified by changing the anion or alkyl chain of the cation. These are used as reaction media in the chemical industry for extraction and fractionations,[13] material preparations,[12,14] synthesis, catalysis, and a host of other applications.[15,16] Several ultrafast spectroscopic and theoretical studies have been investigated in RTILs.[17−30]

In recent years, ionic liquid containing micelles and microemulsions have received much more attention. Long chain ILs contain a charged hydrophilic part and one or more hydrophobic tails, which results in these ILs to form aggregates. This self-aggregation behavior of RTILs in aqueous solution has recently attracted much attention due to its structural similarities with ionic surfactant. The major characteristics such as critical micelle concentration (cmc), aggregation number, and micropolarity of micellar aggregates can be modified by tuning the hydrophobicity of RTILs. Several groups have reported the characterization of RTIL containing micelles and microemulsions.[31−38] Miskolczy et al. showed that, in aqueous medium, 1-butyl-3-methylimidazolium octyl sulfate ($[C_4mim][C_8SO_4]$) forms micelles.[38] Some reports on photophysical studies and solvation dynamics in this RTIL micelle are also available in the literature.[39−41] The special feature of this IL is that its cmc (32−37 mM) in water is quite higher than that of the conventional ionic surfactants.[42] Physical properties of this ionic liquid are well studied. The average hydrodynamic diameter (D_h) of this micelle is ∼2.8 nm.[39] Theoretical calculations[43] on neat $[C_4mim][C_8SO_4]$ show a strong hydrogen bonding between the ion pairs that leads to a fluid structure.

Although several literatures are available on the applications of RTILs as reaction media, sometimes the potential use in

Received: May 25, 2012
Revised: July 11, 2012
Published: July 13, 2012

Scheme 1. Chemical Structures of 3,3′-Diethyloxadicarbocyanine Iodide (DODCI), 1-Butyl-3-methylimidazolium Octyl Sulfate ($[C_4mim][C_8SO_4]$), and *N,N,N*-Trimethyl-*N*-propyl Ammonium Bis(trifluoromethanesulfonyl) Imide, ($[N_{3111}][Tf_2N]$)

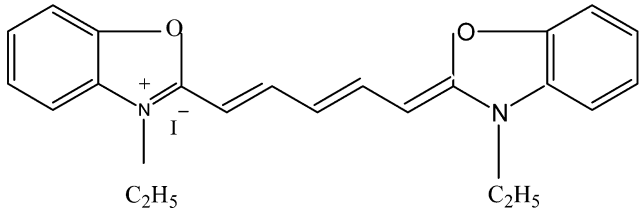

3, 3'-diethyloxadicarbocyanine iodide (DODCI)

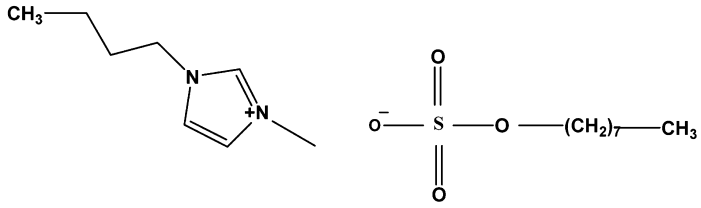

1-butyl-3-methylimidazolium octyl sulfate, $[C_4mim][C_8SO_4]$

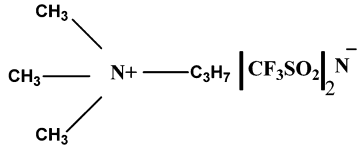

N,N,N–trimethyl-N-propyl ammonium bis(trifluoromethanesulfonyl)imide, $[N_{3111}][Tf_2N]$

chemical reaction is hindered due to some unusual physicochemical property (e.g., high viscosity). The major disadvantage of using RTILs as reaction media is their inability to dissolve solute molecules. This difficulty can be overcome by using suitable polar solvent as a cosolvent. The addition of polar solvent increases the applicability of the RTILs. The mixture of RTILs and conventional solvent is a promising media for spectroscopic and photophysical studies.[44−47] It is found that with the addition of polar solvents in RTILs, polarity,[49,50] viscosity,[51,52] and electrochemical[53] behavior of RTILs changes. Generally, with the addition of cosolvent, viscosity of RTILs decreases. Pandey and co-workers have characterized different RTIL−cosolvent mixtures using various solvatochromic probe molecules.[48,54] Theoretical calculations demonstrated that hydrogen bonding interaction exists between the anion of RTILs and different alcohol.[55] Because of unique features of the RTILs−cosolvent mixture, these systems have been used extensively in solvation dynamics,[56−59] electron transfer reaction,[60] and other ultrafast processes.

In recent years, photoisomerization of organic molecules with conjugated double bonds have been investigated as prototypical examples of unimolecular reactions in the condensed phase.[61,62] The large organic molecules that undergo conformational changes upon optical excitation are an interesting system for the study of solvent influence on excited state decay. Among these, cyanine dyes and other substituted polyenes have been studied extensively.[63−66] In the excited state, the molecules are involved in an activated twist motion about the double bond/bonds to an intermediate geometry. Because of the twist geometry, the energy of the excited state becomes close to the ground state, and it rapidly decays to the twisted ground electronic state by internal conversion. The internal conversion from the twisted excited state is very fast due to a small energy difference between the two states. So, the twisting motion about the double bond or barrier crossing between the excited state and ground state control the nonradiative process. A large molecular motion is required for this isomerization process; thus, it has been controlled by temperature and medium viscosity. The solute−solvent dielectric interaction also governs the isomerization rate due to the polar nature of the transition state. In recent times, photoisomerization have been extensively studied in homogeneous solvent,[64] various organized systems,[67−69] polymer systems,[70,71] and ionic liquids.[72,73]

In the present work, we have studied the photophysics of 3,3′-diethyloxadicarbocyanine iodide (DODCI) in ionic liquid micelle and ionic liquid−cosolvent system. Extensive studies of DODCI have been carried out in different systems to understand the photoisomerization process. Photoisomerization of this dye in alcohols have been investigated in the ground state and excited states by Fleming and co-workers.[63,64] Sitzmann and Eisenthal have investigated the photoisomerization of DODCI at the air−water interface using surface second-harmonic generation techniques.[74] Bhattacharyya and co-workers have further studied the photoisomerization of DODCI in reverse micelles[67] and micelles.[68] It was found that the isomerization rate is faster in the air−water interface compared to bulk water due to reduced friction at the interface, whereas an opposite trend is observed in the micelle−water interface due to increased friction. Mali et al. compared the

dx.doi.org/10.1021/jp305095n | J. Phys. Chem. B 2012, 116, 9482−9491

isomerization rate of DODCI in micellar solution and gel phase of P123, a triblock copolymer.[71] Even though several literatures are available involving photoisomerization in homogeneous solvent,[64,63,75,76] such studies are rare in the ionic liquid system. Mali et al. compared the isomerization rate of two cyanine derivatives in [bmim][PF_6] and aqueous glycerol.[72] It was observed that the nonradiative rate constants of DODCI are almost identical in both the solvent. The finding of this study indicates that viscosity is the main controlling factor for photoisomerization process. Gangamallaiah et al. have examined the photoisomerization in a series of 1-alkyl-3-methylimidazolium (alkyl = methyl, ethyl, propyl, butyl, and hexyl) bis(trifluoromethylsulfonyl) imides[73] to find out the distinct feature of this system compared to other conventional solvent such as alcohols.[75,77] The excited state isomerization of DODCI essentially involves an activated twist motion about the double bonds to an intermediate geometry. The nonradiative process is dominated by this twisting motion or the barrier crossing because internal conversion from the twist excited state is very rapid due to small energy difference between the two states. In the case of DODCI, the nonradiative rate constant essentially represents the rate of photoisomerization, as the contribution from normal the excited state is negligible and the triplet yield is low.[63]

In this article, we have carried out a spectroscopic investigation of DODCI in a micellar system formed by an ionic liquid (IL), 1-butyl-3-methylimidazolium octyl sulfate ([C_4mim][C_8SO_4]) in aqueous medium and also in a binary mixture of another ionic liquid, *N,N,N*-trimethyl-*N*-propyl ammonium bis(trifluoromethanesulfonyl) imide ([N_{3111}][Tf_2N]). The aim of this study is to find out the unique property of RTIL micelle compared to other micelles of conventional surfactant like SDS (sodium dodecyl sulfate). Photoisomerization of DODCI in aromatic RTILs is well studied, but there are no reports concerning nonaromatic RTILs. We have chosen [N_{3111}][Tf_2N], an aprotic nonaromatic RTIL and methanol, acetonitrile, and *n*-propanol as polar cosolvents. Studies on the photophysical properties of DODCI in [N_{3111}][Tf_2N] and its binary mixture with polar solvents indicate that nonradiative rate is mainly controlled by viscosity of the medium.

2. EXPERIMENTAL SECTION

2.1. Materials and Sample Preparation. DODCI (laser grade, Exciton), 2,6-diphenyl-4-(2,4,6-triphenyl-1-pyridinio) phenolate (betaine 30, Sigma-Aldrich), and the ionic liquids, [C_4mim][C_8SO_4] (Fluka) and [N_{3111}][Tf_2N] (Kanto chemical, Japan), were used as received. Methanol, acetonitrile, and *n*-propanol were purchased from Spectrochem, India. Triply distilled Milli-Q water was used to prepare all the micellar solutions. The stock solution of DODCI was prepared in methanol. Appropriate amounts of [C_4mim][C_8SO_4] were weighted in glass bottles, and then, a requisite quantity of water was added. A requisite amount of DODCI was added to the quartz cuvette, and after evaporating methanol, micellar solutions were added. For [N_{3111}][Tf_2N], the RTIL was added to the vial under nitrogen atmosphere and stirred for 10−20 min after removing the methanol under vacuum. Then, the solution was transferred to a quartz cuvette in nitrogen atmosphere and sealed with septum and parafilm. The required amounts of the cosolvents (methanol, acetonitrile, and *n*-propanol) were added and stirred for a few minutes under the nitrogen atmosphere.

The structures of DODCI, [C_4mim][C_8SO_4], and [N_{3111}][Tf_2N] are shown in Scheme 1.

2.2. Instruments and Methods. The absorption and fluorescence spectra were collected using a Shimadzu (model no. UV-1601) UV−vis spectrophotometer and a Hitachi (model no. F-7000) spectrofluorometer, respectively. For steady-state experiments, all the samples were excited at 525 nm, and emission spectra were recorded from 550 to 725 nm. The fluorescence quantum yield in different systems was determined using DODCI in ethanol with a quantum yield of 0.42 at 298 K[66] as a reference. The following equation[77] is used for the calculation of the quantum yield:

$$\frac{\Phi_S}{\Phi_R} = \frac{A_S}{A_R}\frac{(\mathrm{Abs})_R}{(\mathrm{Abs})_S}\frac{{n_S}^2}{{n_R}^2} \quad (1)$$

where Φ represents the quantum yield, Abs represents the absorbance, *A* represents the area under the fluorescence curve, and *n* is the refractive index of the medium. The subscripts S and R denote the corresponding parameters for the sample and reference, respectively.

For steady-state anisotropy measurement, we used a Perkin-Elmer LS-55 luminescence spectrometer equipped with a filter polarizer and a thermostatted cell holder. Steady-state anisotropy is defined as[77]

$$r_0 = \frac{I_{VV} - GI_{VH}}{I_{VV} + 2GI_{VH}} \quad (2)$$

where *G* is the correction factor. I_{VV} and I_{VH} are the fluorescence intensity polarized parallel and perpendicular to the polarization of the excitation light, respectively.

The time-resolved emission spectra were recorded using a TCSPC picosecond spectrophotometer. The samples were excited at 585 nm. The details of the experimental setup for the picosecond TCSPC is described in our previous paper.[78] In brief, a picosecond diode was used as the light source, and the signal was detected in magic angle (54.7°) polarization using a Hamamatsu MCP PMT (3809U). The typical instrument response function is 100 ps in our system. The decays were analyzed using IBH DAS-6 decay analysis software. The temperature was maintained by a circulating water bath.

The average fluorescence lifetimes for the decay curves were calculated from the decay times and the relative contribution of the components using the following equation:[77]

$$\tau_f = a_1\tau_1 + a_2\tau_2 \quad (3)$$

where τ_1 and τ_2 are the first and second components of decay time of the probe, and a_1 and a_2 are the corresponding relative contributation of these components.

2.3. Viscosity Measurement. The viscosity of the 100 mM [C_4mim][C_8SO_4], neat [N_{3111}][Tf_2N] at different temperatures, and [N_{3111}][Tf_2N]−cosolvent mixture was measured using a Brookfield DV-II+ Pro (viscometer). The temperature was maintained by a circulating water bath (RW-0525G).

3. RESULTS AND DISCUSSION

3.1. Steady-State Results. DODCI exhibits a strong absorption peak around 576 nm in water and 581 nm in neat [N_{3111}][Tf_2N]. The absorption spectra of this dye is red-shifted by about ∼12 nm in 100 mM [C_4mim][C_8SO_4] solution than water. This is due to the encapsulation of DODCI in the micellar phase similar to that observed in the case of other micellar systems.[68,71] A similar trend is observed in the case of

dx.doi.org/10.1021/jp305095n | J. Phys. Chem. B 2012, 116, 9482−9491

emission spectra (Table 1). The normalized absorption and emission spectra of DODCI in water, neat $[N_{3111}][Tf_2N]$, and

Table 1. Absorption and Emission Maxima with Change of $[C_4mim][C_8SO_4]$ Concentration

concentration (mM)	λ_{abs}^{max} (nm)[a]	λ_{em}^{max} (nm)[a]
0	576	600
38	587	613
100	588	614

[a]Experimental error ±2 nm.

100 mM $[C_4mim][C_8SO_4]$ are shown in Figures 1 and 2, respectively. This shift in the spectra occurs due to a change in the polarity of the medium from water to micelle.

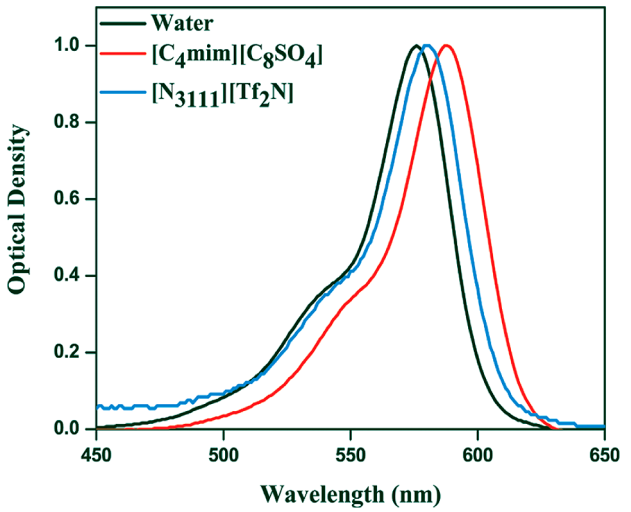

Figure 1. Absorption spectra of DODCI in water, 100 mM $[C_4mim][C_8SO_4]$ solution, and neat $[N_{3111}][Tf_2N]$.

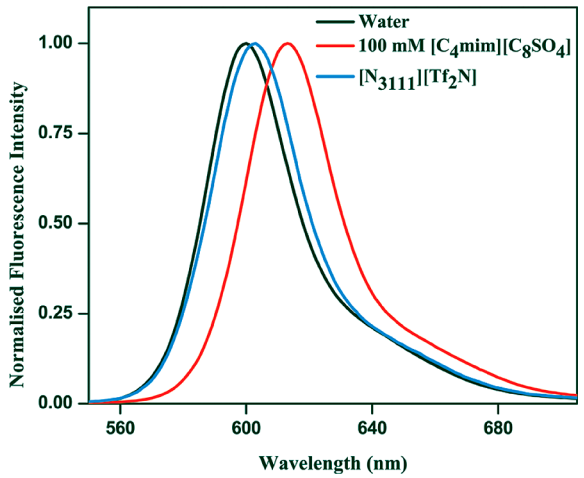

Figure 2. Emission spectra of DODCI in water, 100 mM $[C_4mim][C_8SO_4]$ solution, and neat $[N_{3111}][Tf_2N]$.

3.1.1. $[C_4mim][C_8SO_4]$ Micelle. In aqueous solution, DODCI shows strong fluorescence with the emission maximum at 600 nm and quantum yield of ~0.29. With the addition of $[C_4mim][C_8SO_4]$, significant spectral changes are observed, as shown in Figure 3. At the lower concentrations of RTILs, the absorbance at 580 nm decreases, the spectra become broader due to the increase of the shoulder absorbance at 560 nm and also the emission intensity decreases. Below the cmc, the changes in the absorption and emission spectra indicate the formation of complexes between the positively charged DODC and negatively charged $[C_8SO_4]$. This observation is completely in line with the earlier observations in anionic (sodium dodecyl sulfate, SDS) micelle.[68] Above the cmc of $[C_4mim][C_8SO_4]$, the absorption and emission intensity increases due to the partition of probe molecules in the micellar phase. For better understanding of the photophysics of DODCI, we have also determined the change in fluorescence quantum yield (Φ) with increasing $[C_4mim][C_8SO_4]$ concentration. Variation of quantum yield of DODCI with IL concentration is shown in Figure 4. Upon the addition of IL to aqueous solution containing DODCI, initially, the quantum yield decreases to ~0.25 in 7 mM solution, then it increases to ~0.40 in 100 mM solution. The change of Φ is sharp around the cmc of $[C_4mim][C_8SO_4]$, and it reaches saturation after the cmc value. The increase of Φ value with the increase in concentration of IL (near the cmc range) is a clear evidence of the suppression of the nonradiative pathway, i.e., the photoisomerization rate of DODCI in the $[C_4mim][C_8SO_4]$ micelle.

Steady-state anisotropy (r_0) measurement provides fruitful information about the restriction imposed by the microheterogenous media on the degree of rotation of DODCI molecule.[77,79−81] With the addition of IL, a gradual increment in anisotropy is observed followed by a plateau at higher concentration by using eq 2. The steady-state anisotropy value of DODCI in water is ~0.09, but in 100 mM $[C_4mim][C_8SO_4]$, the anisotropy becomes ~0.13. As depicted in Figure 5, an increase in anisotropy with an increase in IL concentration reflects the increased rigidity of the microenvironment experienced by the probe molecules. A high value of anisotropy above the cmc indicates that the probe molecules are held rigidly inside the micellar region.

3.1.2. Ionic Liquid−Cosolvent Mixture. Steady-state fluorescence measurements are carried out to determine the fluorescence quantum yield of DODCI with the variation of ionic liquid−cosolvent composition. The emission spectra of DODCI shows a strong peak at ~603 nm in neat $[N_{3111}][Tf_2N]$. With gradual addition of cosolvent, i.e, methanol, acetonitrile, and *n*-propanol, the emission peak remains unaffected, but the emission intensity gradually decreases. The representative emission spectra of DODCI in $[N_{3111}][Tf_2N]$−cosolvent mixtures and variation of quantum yield with the mole fraction of cosolvent are depicted in Figure 6. The observed emission peak in $[N_{3111}][Tf_2N]$ is very close to the emission peak in ethanol (~602 nm). It indicates that the polarity of this ionic liquid is very close to ethanol. The observed Φ of DODCI in neat ionic liquid is very high by 0.85 at 298 K due to the high viscosity of $[N_{3111}][Tf_2N]$ that inhibits the twisting motion around the double bond and causes the retardation of photoisomerization rate. With the addition of 0.50 mol fraction of methanol, acetonitrile, and *n*-propanol, the emission quantum yield decreases to 0.71, 0.67, and 0.64, respectively.

The polarity of $[N_{3111}][Tf_2N]$ will also change with the addition of a polar solvent. To get an idea about the polarity of the system, we have utilized one of the most typical polarity probes, betaine 30 ($E_T(30)$),[82,83] to measure the polarity. $E_T(30)$ probe has been widely used by many groups to characterized the microheterogenous media.[18,37,54,82−86] We

dx.doi.org/10.1021/jp305095n | J. Phys. Chem. B 2012, 116, 9482−9491

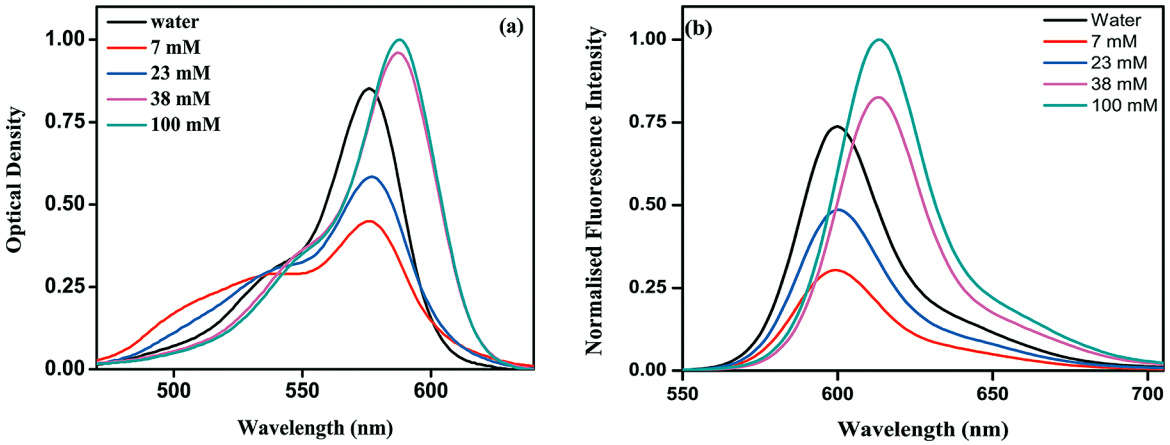

Figure 3. Steady-state (a) absorption and (b) emission spectra of DODCI aqueous solution with increasing concentration of $[C_4mim][C_8SO_4]$.

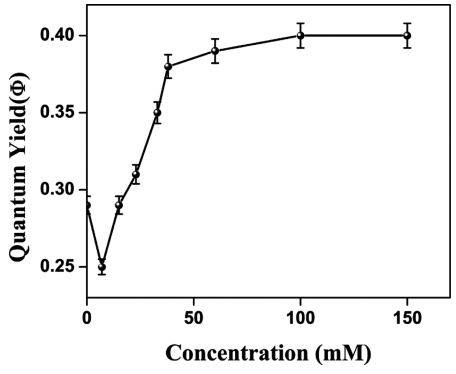

Figure 4. Variation of quantum yield (Φ) with increasing concentration of $[C_4mim][C_8SO_4]$ in aqueous solution.

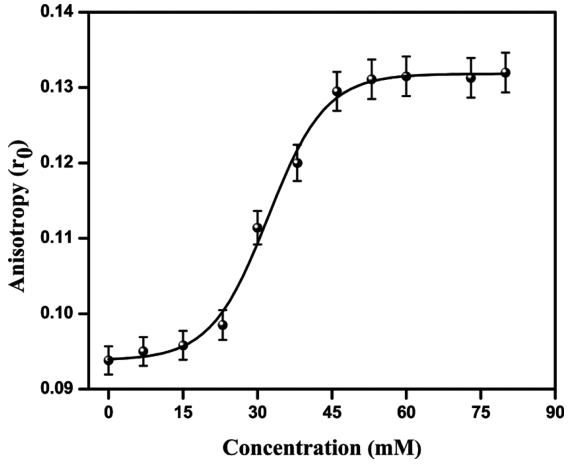

Figure 5. Change of steady-state fluorescence anisotropy (r_0) with increasing concentration of $[C_4mim][C_8SO_4]$ in aqueous solution.

have also determined the $E_T(30)$ value using the following equation.

$$E_T(30) = hc\nu_{max}N_A = \frac{28591}{\lambda_{max}(\text{nm})}\frac{\text{kcal}}{\text{mol}} \quad (4)$$

In this equation h, c, and N_A are Planck's constant, velocity of light, and Avogadro's number, respectively. λ_{max} and ν_{max} are the wavelength (in nm) and frequency of the maximum absorption of the $E_T(30)$ probe, respectively. The absorption spectra of $E_T(30)$ probe in $[N_{3111}][Tf_2N]$−cosolvent systems are shown in Figure S1 (Supporting Information), which clearly shows that the absorption maxima (λ_{max}) are blue-shifted with the addition of cosolvent. The variations of polarity with the addition of cosolvents are shown in Figure 7. In neat $[N_{3111}][Tf_2N]$, the $E_T(30)$ value is about ∼50.61 kcal/mol. As depicted in Figure 7, with the addition of 0.50 mol fraction of methanol and *n*-propanol, the $E_T(30)$ value increases to ∼54.67 kcal/mol and ∼53.14 kcal/mol, respectively, but with the addition of acetonitrile, it remains almost constant.

3.2. Time-Resolved Results. Besides the steady-state measurements, time-resolved fluorescence measurements are also necessary to get an idea about the photoisomerization process. Fluorescence lifetime serves as an indicator to explore the environment around a fluorophore.[79−81,87] Here, we have monitored the fluorescence lifetime of DODCI with the increasing concentration of $[C_4mim][C_8SO_4]$ and different $[N_{3111}][Tf_2N]$−cosolvent composition.

3.2.1. [C₄mim][C₈SO₄] Micelle. The time-resolved fluorescence decays of DODCI in aqueous solution with varying concentration of $[C_4mim][C_8SO_4]$ are recorded at the excitation wavelength of 585 nm. Time-resolved emission decay in aqueous solution fits well to a single exponential function with a time constant of ∼63 ps, which matches the reported value in the literature.[68] In contrast, the decays in micellar solution are fitted with the following biexponential function:

$$f(t) = a_1e^{-t/\tau_1} + a_2e^{-t/\tau_2} \quad (5)$$

Fluorescence decay profiles of DODCI at different concentrations of $[C_4mim][C_8SO_4]$ are shown in Figure 8. After the cmc, the average lifetime of DODCI increases due to entrapment of probe molecules in the micellar system. The lifetime components in the 100 mM micellar system are ∼1.43 ns (98%) and ∼0.75 ns (2%). The probe molecule dissolved in micellar medium can be solubilized in bulk water, interfacial region, Stern layer, and core. Neutral solute are generally located in the Stern layer and charged ones at the micelle−water interface or even in bulk water. DODCI, a cationic probe, is expected to be solubilized in the micelle−water interface or in bulk water. The experimentally measured lifetime values of DODCI in 100 mM solution are ∼1.43 ns (98%) and ∼0.75 ns (2%), but in bulk water, the lifetime of DODCI is ∼0.63 ns. The lifetime values of the probe confined in the micellar environment are significantly longer than those observed in water. These finding suggest that the probes are not solubilized

dx.doi.org/10.1021/jp305095n | J. Phys. Chem. B 2012, 116, 9482−9491

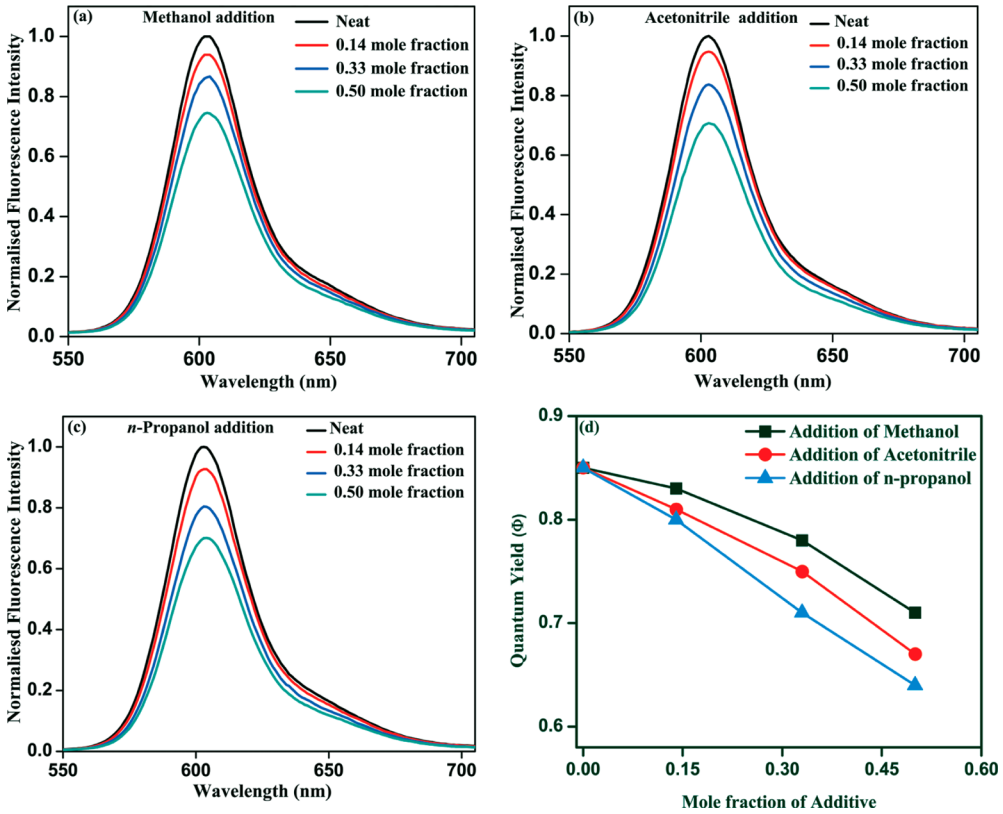

Figure 6. Steady-state fluorescence spectra of DODCI in $[N_{3111}][Tf_2N]$−cosolvent system: (a) addition of methanol, (b) addition of acetonitrile, (c) addition of *n*-propanol, and (d) variation of quantum yield (Φ) with mole fraction of cosolvent.

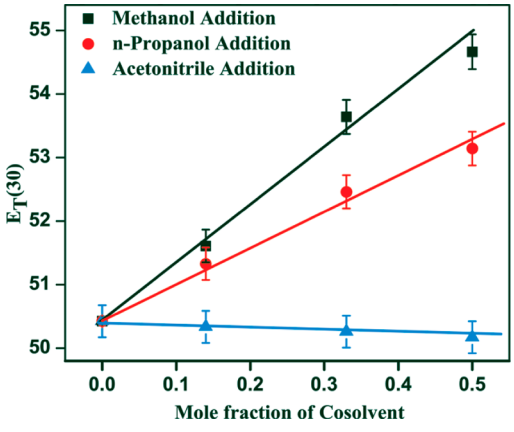

Figure 7. Variation of polarity of $[N_{3111}][Tf_2N]$−cosolvent system.

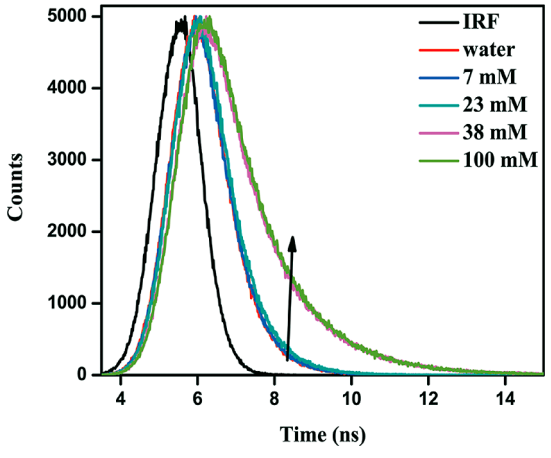

Figure 8. Time-resolved decay plot of DODCI with change in concentration of $[C_4mim][C_8SO_4]$.

in bulk water surrounding the micelles. These data indicate that the probes are solubilized in two regions in 100 mM $[C_4mim][C_8SO_4]$ solution. The lifetime of DODCI is strongly dependent on the nonradiative rate. So the longer lifetime component can be assigned to the probe located in the Stern layer and the shorter ones due to the location of the probe in micelle−water interface. The observed result is due to the higher microviscosity of the Stern layer than that of the micelle−water interface. From the pre-exponential factors of fluorescence decays, it is clear that 96−98% of the probes are solubilized in the Stern layer and only 2−4% at the micelle−water interface. This result indicates that the positive charge on DODCI pointing toward the bulk water and the hydrocarbon portion sticking into the micellar aggregates. We have also calculated the average lifetime (τ_f) by using eq 3 to explain the excited-state dynamic processes. The average lifetime of DODCI is increased by 2.25 times in 100 mM $[C_4mim]$-$[C_8SO_4]$ solution compared to water.

The photophysics of DODCI is dominated by a very fast isomerization process, which occurs from the fast singlet excited states. Because of optical excitation, the bond order along the polymethine chain gets reduced, and it forms a twist intermediate geometry. This twisted state rapidly undergoes internal conversion to the ground electronic state. Flash photolysis studies reveal that isomerization is the dominant pathway for the nonradiative decay for the DODCI molecule.[64] As the triplet quantum yields for these molecules are small, k_{isc} can be neglected compared to (k_{ic} + k_{isc}). Thus, the k_{nr} of

dx.doi.org/10.1021/jp305095n | J. Phys. Chem. B 2012, 116, 9482−9491

Table 2. Quantum Yield (Φ), Fluorescence Lifetime (τ_f), and Radiative (k_r) and Nonradiative Rate (k_{nr}) Constants of DODCI in Aqueous Solution with Increasing Concentration of $[C_4mim][C_8SO_4]$

conc. (mM)	quantum yield (Φ)	$\tau_1(a_1)$ (ns)	$\tau_2(a_2)$ (ns)	τ_f (ns)	k_r (10^9 s^{-1})	k_{nr} (10^9 s^{-1})
0	0.29		0.63	0.63 ± 0.03	0.460	1.127
38	0.38	1.43(0.91)	0.74(0.09)	1.37 ± 0.05	0.277	0.452
100	0.40	1.43(0.98)	0.75(0.02)	1.42 ± 0.06	0.282	0.422

DODCI has been identified as the rate of isomerization about the double bond.[62,64,88]

The changes in fluorescence lifetime values with the gradual addition of IL help us to get an idea about the radiative nonradiative decay processes through entrapment of probe molecules. The radiative and nonradiative rate constants were calculated from the determined fluorescence quantum yield (Φ) and average fluorescence lifetime (τ_f) using the following equations:

$$k_r = \frac{\Phi}{\langle \tau_f \rangle} \tag{6}$$

$$k_{nr} = \frac{1}{\langle \tau_f \rangle} - k_r \tag{7}$$

where k_r and k_{nr} represent the radiative and nonradiative rate constants, respectively. The calculated values are given in Table 2. In water, the nonradiative rate constant of DODCI is very high ~1.127×10^9 s^{-1}. The k_{nr} value is reduced with an increasing effect of confinement. The nonradiative rate constant in the micelle is ~0.422×10^9 s^{-1}. The decrease of nonradiative rate constant by 2.69 times near cmc range indicates the confinement of probe molecules in the micellar phase. In the micellar environment due to higher microviscosity, twisting motion around the double bond/bonds decreases. So, the enhanced fluorescence intensity along with an increase in lifetime in the 100 mM $[C_4mim][C_8SO_4]$ solution, compared with pure aqueous solution, is consistent with the decrease in the nonradiative decay channels in this restricted environment.

3.2.2. Ionic Liquid–Cosolvent Mixture. Viscosity of the medium is an important parameter in controlling the rate of photoisomerization processes. So, we have monitored the time-resolved fluorescence decays in different $[N_{3111}][Tf_2N]$–cosolvent composition. The representative fluorescence decays of DODCI in neat $[N_{3111}][Tf_2N]$ and after addition of 0.50 mol fraction cosolvent (methanol, acetonitrile, and *n*-propanol) are shown in Figure S2 (Supporting Information). The observed lifetime of DODCI in neat $[N_{3111}][Tf_2N]$ is 1.48 ns. The lifetime is much higher compared to water (~63 ps). Thus, it is clear that the rate of photoisomerization of DODCI is drastically retarded in IL compared to water. Upon gradual addition of 0.50 mol fraction cosolvent (methanol, acetonitrile, and *n*-propanol), the photoisomerization rate increases and the lifetime of DODCI decreases to 1.27, 1.16, and 1.22 ns, respectively. The high viscosity of $[N_{3111}][Tf_2N]$ inhibits the twisting motion about the double bonds of DODCI and causes the drastic retardation of photoisomerization rate.

To comprehend the photoisomerization process of these systems, the radiative rate constant (k_r) and nonradiative rate constant (k_{nr}) were obtained using eqs 6 and 7. The observed nonradiative rate in neat ionic liquid (0.102×10^9 s^{-1}) is 11 times slower compared to water (1.13×10^9 s^{-1}). Fluorescence quantum yields, average lifetimes, and radiative and nonradiative rate constants of DODCI in $[N_{3111}][Tf_2N]$–cosolvent mixtures are summarized in Table 3. The viscosity of neat $[N_{3111}][Tf_2N]$ is quite high (~69 cP at 298 K). We have measured the polarity and viscosity of different RTIL–cosolvent mixtures. The addition of cosolvent in neat $[N_{3111}][Tf_2N]$ decreases the viscosity. The presence of cosolvent molecules reduces the electrostatic attraction between the ions. The –OH moiety of the alcohol forms a hydrogen bond with the anion of the RTIL moiety.[56,57] The addition of polar solvent also separates the cations and anions of RTILs, i.e, decreases the overall cohesive energy, resulting in a decrease in viscosity. The addition of 0.50 mol fraction of cosolvent (methanol, acetonitrile, and *n*-propanol) the nonradiative rate becomes 0.228×10^9 s^{-1}, 0.284×10^9 s^{-1} ,and 0.295×10^9 s^{-1}, respectively. The decrease in viscosity increases the twisting motion around the double bonds of DODCI; as a result, the nonradiative rate, i.e., rate of photoisomerization, increases. The observed trend in nonradiative rate constant in $[N_{3111}][Tf_2N]$–cosolvent system indicates that viscosity is the controlling factor in the photoisomerization process. If polarity controls over viscosity, then we observed opposite trend in isomerization rate constant between $[N_{3111}][Tf_2N]$–alcohol and $[N_{3111}][Tf_2N]$–acetonitrile system.

Table 3. Quantum Yield (Φ), Fluorescence Lifetime (τ_f), and Radiative (k_r) and Nonradiative Rate (k_{nr}) Constants of DODCI in $[N_{3111}][Tf_2N]$–Cosolvent System

system	mole fraction	quantum yield (Φ)	$\langle \tau_f \rangle$ (ns)	k_r (10^9 s^{-1})	k_{nr} (10^9 s^{-1})
$[N_{3111}][Tf_2N]$	0	0.85	1.48 ± 0.07	0.574	0.102
$[N_{3111}][Tf_2N]$ + methanol	0.14	0.83	1.43 ± 0.06	0.580	0.119
	0.33	0.78	1.36 ± 0.05	0.574	0.161
	0.50	0.71	1.27 ± 0.05	0.559	0.228
$[N_{3111}][Tf_2N]$ + acetonitrile	0.14	0.81	1.35 ± 0.05	0.600	0.141
	0.33	0.75	1.25 ± 0.05	0.600	0.200
	0.50	0.67	1.16 ± 0.04	0.578	0.284
$[N_{3111}][Tf_2N]$ + *n*-propanol	0.14	0.80	1.36 ± 0.05	0.588	0.147
	0.33	0.71	1.28 ± 0.05	0.555	0.226
	0.50	0.64	1.22 ± 0.04	0.525	0.295

3.3. Viscosity Measurement. We measured the viscosity of $[N_{3111}][Tf_2N]$–cosolvent mixtures. The bulk viscosities of $[N_{3111}][Tf_2N]$–cosolvent mixtures gradually decreases with the addition of polar solvent. We also measured the viscosity of 100 mM $[C_4mim][C_8SO_4]$ micellar solution and neat $[N_{3111}][Tf_2N]$ at six different temperatures (Table 4). The bulk viscosity of $[N_{3111}][Tf_2N]$–cosolvent mixture are tabulated in Table 5.

4. TEMPERATURE-DEPENDENT STUDY

Temperature-dependent fluorescence provides fruitful information about the dependence of the nonradiative process on the viscosity of the medium. The increase in temperature from 293 K to 318 K, the fluorescence intensity of DODCI decreases sharply in 100 mM $[C_4mim][C_8SO_4]$ micellar solution and also in neat $[N_{3111}][Tf_2N]$, as shown in Figure S3 (Supporting Information). With an increase in temperature, the nonradiative

dx.doi.org/10.1021/jp305095n | J. Phys. Chem. B 2012, 116, 9482–9491

Table 4. Bulk Viscosity of 100 mM $[C_4mim][C_8SO_4]$ and Neat $[N_{3111}][Tf_2N]$ at Different Temperature

system	viscosity (cp)[a]					
	293 K	298 K	303 K	308 K	313 K	318 K
100 mM $[C_4mim][C_8SO_4]$	1.07	0.98	0.92	0.86	0.80	0.75
Neat $[N_{3111}][Tf_2N]$	86	69	57	46	38	32

[a]Experimental error ~5%.

Table 5. Bulk Viscosity of $[N_{3111}][Tf_2N]$−Cosolvent Mixture

system	mole fraction	viscosity (cp)[a]
$[N_{3111}][Tf_2N]$ + methanol	0.14	52
	0.33	39
	0.50	20
$[N_{3111}][Tf_2N]$ + acetonitrile	0.14	48
	0.33	26
	0.50	18
$[N_{3111}][Tf_2N]$ + *n*-propanol	0.14	48
	0.33	36
	0.50	22

[a]Experimental error 5%.

rate constant increases, and consequently, quantum yield decreases (Figure 9). To determine the activation energy for

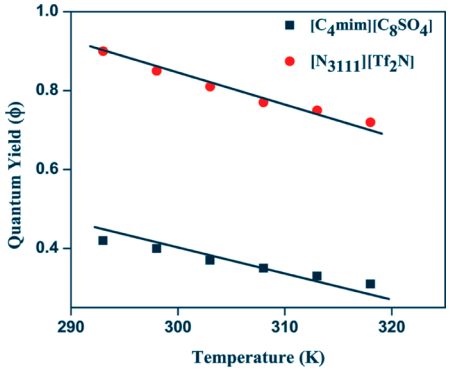

Figure 9. Variation of quantum yield (Φ) of DODCI in 100 mM $[C_4mim][C_8SO_4]$ and neat $[N_{3111}][Tf_2N]$ as a function of temperature.

the photoisomerization process, we have calculated the radiative and nonradiative rate using eqs 6 and 7 at different temperatures, and the results are tabulated in Tables 6 and 7 for 100 mM $[C_4mim][C_8SO_4]$ and neat $[N_{3111}][Tf_2N]$, respectively. The fluorescence decays of DODCI in 100 mM $[C_4mim][C_8SO_4]$ and neat $[N_{3111}][Tf_2N]$ at different temperatures are shown in Figure 10. From the Arrhenius plot (Figure

Table 7. Quantum Yield (Φ), Fluorescence Lifetime (τ_f), and Radiative (k_r) and Nonradiative Rate (k_{nr}) Constants of DODCI in Neat $[N_{3111}][Tf_2N]$ As a Function of Temperature

temperature (K)	quantum yield (Φ)	$\langle\tau_f\rangle$ (ns)	k_r (10^9 s^{-1})	k_{nr} (10^9 s^{-1})
293	0.90	1.55 ± 0.07	0.581	0.064
298	0.85	1.48 ± 0.06	0.574	0.102
303	0.81	1.41 ± 0.06	0.574	0.135
308	0.77	1.34 ± 0.05	0.575	0.171
313	0.75	1.25 ± 0.05	0.600	0.200
318	0.73	1.18 ± 0.04	0.619	0.288

11) we have calculated the activation energy (E_a) and the preexponential factor (A) for the photoisomerization process of DODCI. The calculated activation energy for 100 mM $[C_4mim][C_8SO_4]$ solution and neat $[N_{3111}][Tf_2N]$ are, respectively, ~4.47 kcal/mol and ~9.25 kcal/mol (Table 8). From the ln k_{nr} versus $1/T$ plot, we have calculated activation energy; it cannot be estimated from such plots due to expected influence of temperature on viscosity. For this purpose, isoviscous plots in a homologous series of solvents are often employed. The barrier heights are also dependent on the polarity of the medium because of the polar nature of the transition state involved in the isomerization reactions. To minimize the effect of viscosity and polarity on the isomerization rate constants and activation energies of the reaction, nonradiative rate constants were measured under isoviscous and isodielectric conditions, and modified Kramers' equation[64] has been employed for homologous series of solvent. Activation energy of a reaction is usually obtained by using the Arrhenius law from the temperature dependent rate constants. To maintain isoviscous conditions, Arrhenius plots have been constructed for the nonradiative rate where solvent viscosity is kept constant while the temperature and member of the homologous series are varied.[73,89]

However, to get the qualitative idea about the activation energy, we have used a temperature dependent study in the 100 mM $[C_4mim][C_8SO_4]$ solution and neat $[N_{3111}][Tf_2N]$ systems. In our experimental temperature range (293−318 K), it has been observed a linear plot between ln k_{nr} and $1/T$.[63] These results indicate that the calculated activation energy corresponds to the ground state activation energy.

5. CONCLUSIONS

In this study, we have reported on the modulation of photophysics of DODCI in RTIL micelle and RTIL−cosolvent mixture. The photoisomerization rate is drastically hindered in 100 mM $[C_4mim][C_8SO_4]$ micellar solution and $[N_{3111}][Tf_2N]$−cosolvent binary mixture compared to water. The hydrophobic and confined environments provided by micelles

Table 6. Quantum Yield (Φ), Fluorescence Lifetime (τ_f), and Radiative (k_r) and Nonradiative Rate (k_{nr}) Constants of DODCI in 100 mM $[C_4mim][C_8SO_4]$ Micellar Solution As a Function of Temperature

temperature (K)	quantum yield (Φ)	$\tau_1(a_1)$ (ns)	$\tau_2(a_2)$ (ns)	τ_f (ns)	k_r (10^9 s^{-1})	k_{nr} (10^9 s^{-1})
293	0.42	0.80(0.04)	1.58(0.96)	1.55 ± 0.07	0.271	0.362
298	0.40	0.74(0.05)	1.43(0.95)	1.40 ± 0.06	0.286	0.428
303	0.37	0.71(0.06)	1.36(0.94)	1.32 ± 0.05	0.280	0.478
308	0.35	0.65(0.05)	1.24(0.95)	1.22 ± 0.05	0.287	0.533
313	0.33	0.61(0.05)	1.13(0.95)	1.10 ± 0.04	0.300	0.609
318	0.31	0.55(0.04)	1.04(0.96)	1.02 ± 0.04	0.304	0.676

dx.doi.org/10.1021/jp305095n | J. Phys. Chem. B 2012, 116, 9482−9491

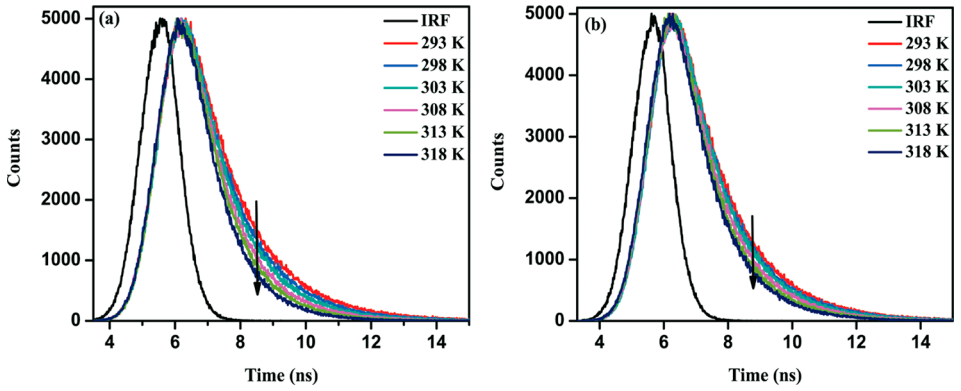

Figure 10. Time-resolved decay plot of DODCI in (a) 100 mM $[C_4mim][C_8SO_4]$ and (b) neat $[N_{3111}][Tf_2N]$ as a function of temperature.

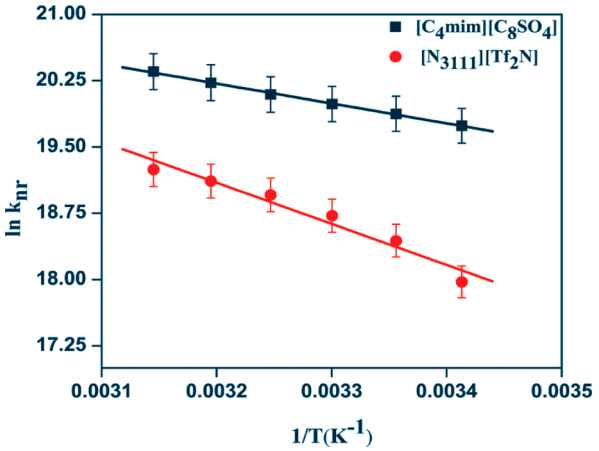

Figure 11. Plot of ln k_{nr} vs $1/T$ for DODCI in 100 mM $[C_4mim][C_8SO_4]$ and neat $[N_{3111}][Tf_2N]$.

Table 8. Activation Energy Parameters

system	activation energy, E_a (kcal/mol)	ln A
100 mM $[C_4mim][C_8SO_4]$	4.47	27.42
Neat $[N_{3111}][Tf_2N]$	9.25	33.98

result in an increase in fluorescence quantum yield and lifetime of DODCI. DODCI is a cationic probe; it is expected to be solubilized at the interface, but from time-resolved measurement, it has been found that a majority of DODCI is located in the Stern layer of micelles. The isomerization rate in the Stern layer of the micelles is slower compared to interface. This is due to the higher microviscosity experienced by the probe in the micellar interior. The photoisomerization rate of DODCI in $[N_{3111}][Tf_2N]$ is drastically retarded. This is due to high viscosity of the neat $[N_{3111}][Tf_2N]$. The addition of cosolvent in $[N_{3111}][Tf_2N]$ screen the electrostatic attraction between the cations and the anions of RTILs. As a result, the bulk viscosity of $[N_{3111}][Tf_2N]$ gradually decreases with the addition of cosolvent. The decrease in viscosity offers less friction to the isomerization process. We have also measured the polarity of RTIL–cosolvent binary mixture using $E_T(30)$ as a molecular probe. As the photoisomerization rate increases with the addition of cosolvent, we can conclude that polarity has less influence compared to viscosity on the photoisomerization of DODCI.

■ ASSOCIATED CONTENT

Supporting Information

Information on the change in absorption spectra of $E_T(30)$, fluorescence decays of DODCI in in $[N_{3111}][Tf_2N]$–cosolvent system, and emission spectra of DODCI in $[C_4mim][C_8SO_4]$ and $[N_{3111}][Tf_2N]$–cosolvent. This material is available free of charge via the Internet at http://pubs.acs.org.

■ AUTHOR INFORMATION

Corresponding Author

* Fax: 91-3222-255303. E-mail: nilmoni@chem.iitkgp.ernet.in.

Notes

The authors declare no competing financial interest.

■ ACKNOWLEDGMENTS

N.S. is thankful to the Council of Scientific and Industrial Research (CSIR) Board of Research in Nuclear Sciences (BRNS), Government of India, for generous research grants. S.G., S.M., and V.G.R. are thankful to CSIR for a research fellowship. C.B. is thankful to UGC for a research fellowship.

■ REFERENCES

(1) Rogers, R. D.; Seddon, K. R. *Science* **2003**, *302*, 792–793.
(2) Haumann, M.; Riisager, A. *Chem. Rev.* **2008**, *108*, 1474–1497.
(3) Parvulescu, V. I.; Hardacre, C. *Chem. Rev.* **2007**, *107*, 2615–2665.
(4) Lee, S.-G. *Chem. Commun.* **2006**, 1049–1063.
(5) Anderson, J. L.; Armstrong, D. W. *Anal. Chem.* **2003**, *75*, 4851–4858.
(6) Baker, G. A.; Baker, S. N.; Pandey, S.; Bright, F. V. *Analyst* **2005**, *130*, 800–808.
(7) Baker, G. A.; Baker, S. N. *Aust. J. Chem.* **2005**, *58*, 174–177.
(8) Ding, J.; Welton, T.; Armstrong, D. W. *Anal. Chem.* **2004**, *76*, 6819–6822.
(9) Welton, T. *Chem. Rev.* **1999**, *99*, 2071–2084.
(10) Welton, T. *Coord. Chem. Rev.* **2004**, *248*, 2459–2477.
(11) Hagiwara, R.; Ito, Y. *J. Fluorine Chem.* **2000**, *105*, 221–227.
(12) Dupont, J.; de Souza, R. F.; Suarez, P. A. Z. *Chem. Rev.* **2002**, *102*, 3667–3691.
(13) Earle, M. J.; Seddon, K. R.; McCormac, P. B. *Green Chem.* **2000**, *2*, 261–262.
(14) Wasserscheid, P.; Welton, T. *Ionic Liquids in Synthesis*; Wiley-VCH: Weinheim, Germany, 2002.
(15) Cole, A. C.; Jensen, J. L.; Ntai, I.; Tran, K. L. T.; Weaver, K. J.; Forbes, D. C., Jr.; Davis, J. H. *J. Am. Chem. Soc.* **2002**, *124*, 5962–5963.
(16) Brown, R. A.; Pollet, P.; McKoon, E.; Eckert, C. A.; Liotta, C. L.; Jessop, P. G. *J. Am. Chem. Soc.* **2001**, *123*, 1254–1255.
(17) Aki, S. N. V. K.; Brennecke, J. F.; Samanta, A. *Chem. Commun.* **2001**, 413–414.
(18) Reichardt, C. *Green Chem.* **2005**, *7*, 339–351.

(19) Karmakar, R.; Samanta, A. *J. Phys. Chem. A* **2002**, *106*, 4447−4452.
(20) Saha, S.; Mandal, P. K.; Samanta, A. *Phys. Chem. Chem. Phys.* **2004**, *6*, 3106−3110.
(21) Adhikari, A.; Sahu, K.; Dey, S.; Ghosh, S.; Mandal, S.; Bhattacharyya, K. *J. Phys. Chem. B* **2007**, *111*, 12809−12816.
(22) Ito, N.; Arzhantsev, S.; Heitz, M.; Maroncelli, M. *J. Phys. Chem. B* **2004**, *108*, 5771−5777.
(23) Arzhantsev, S.; Ito, N.; Heitz, M.; Maroncelli, M. *Chem. Phys. Lett.* **2003**, *381*, 278−286.
(24) Arzhantsev, S.; Jin, H.; Baker, G. A.; Maroncelli, M. *J. Phys. Chem. B* **2007**, *111*, 4978−4989.
(25) Chowdhury, P. K.; Halder, M.; Sanders, L.; Calhoun, T.; Anderson, J. L.; Armstrong, D. W.; Song, X.; Petrich, J. W. *J. Phys. Chem. B* **2004**, *108*, 10245−10255.
(26) Mukherjee, P.; Crank, J. A.; Halder, M.; Armstrong, D. W.; Petrich, J. W. *J. Phys. Chem. A* **2006**, *110*, 10725−10730.
(27) Castner, E. W., Jr.; Wishart, J. F.; Shirota, H. *Acc. Chem. Res.* **2007**, *40*, 1217−1227.
(28) Chakrabarty, D.; Chakraborty, A.; Seth, D.; Hazra, P.; Sarkar, N. *Chem. Phys. Lett.* **2004**, *397*, 469−474.
(29) Chakrabarty, D.; Chakraborty, A.; Seth, D.; Sarkar, N. *J. Phys. Chem. A* **2005**, *109*, 1764−1769.
(30) Shirota, H.; Castner, E. W., Jr. *J. Phys. Chem. B* **2005**, *109*, 21576−21585.
(31) Gao, H.; Li, J.; Han, B.; Chen, W.; Zhang, J.; Zhang, R.; Yan, D. *Phys. Chem. Chem. Phys.* **2004**, *6*, 2914−2916.
(32) Cheng, S.; Zhnag, J.; Zhang, Z.; Han, B. *Chem. Commun.* **2007**, 2497−2499.
(33) Gao, Y.; Han, S.; Han, B.; Li, G.; Shen, D.; Li, Z.; Du, J.; Hou, W.; Zhang, G. *Langmuir* **2005**, *21*, 5681−5684.
(34) Fletcher, K. A.; Pandey, S. *Langmuir* **2004**, *20*, 33−36.
(35) Pramanik, R.; Sarkar, S.; Ghatak, C.; Rao, V. G.; Setua, P.; Sarkar, N. *J. Phys. Chem. B* **2010**, *114*, 7579−7586.
(36) Pramanik, R.; Ghatak, C.; Rao, V. G.; Sarkar, S.; Sarkar, N. *J. Phys. Chem. B* **2011**, *115*, 5971−5979.
(37) Rao, V. G.; Ghosh, S.; Ghatak, C.; Mandal, S.; Brahmachari, U.; Sarkar, N. *J. Phys. Chem. B* **2012**, *116*, 2850−2855.
(38) Miskolczy, Z.; Sebok-Nagy, K.; Biczok, L.; G€okturk, S. *Chem. Phys. Lett.* **2004**, *400*, 296−300.
(39) Seth, D.; Sarkar, S.; Sarkar, N. *Langmuir.* **2008**, *24*, 7085−7091.
(40) Ghatak, C.; Rao, V. G.; Mandal, S.; Ghosh, S.; Sarkar, N. *J. Phys. Chem. B* **2012**, *116*, 3369−3379.
(41) Sarkar, S.; Mandal, S.; Pramanik, R.; Ghatak, C.; Rao, V. G.; Sarkar, N. *J. Phys. Chem. B* **2011**, *115*, 6100−6110.
(42) Heintza, A.; Lehmanna, J. K.; Kozlovab, S. A.; Balantsevac, E. V.; Bazylevad, A. B.; Ondoe, D. *Fluid Phase Equilib.* **2010**, *294*, 187−196.
(43) Davila, M. J.; Aparicio, S.; Alcalde, R.; Garcia, B.; Leal, J. M. *Green Chem.* **2007**, *9*, 221−232.
(44) Hu, Z.; Huang, X.; Annapureddy, H. V. R.; Margulis, C. J. *J. Phys. Chem. B* **2008**, *112*, 7837−7849.
(45) Santhosh, K.; Samanta, A. *J. Phys. Chem. B* **2010**, *114*, 9195−9200.
(46) Kashyap, H. K.; Biswas, R. *J. Phys. Chem. B* **2010**, *114*, 254−268.
(47) Page, T. A.; Kraut, N. D.; Page, P. M.; Baker, G. A.; Bright, F. V. *J. Phys. Chem. B* **2009**, *113*, 12825−12830.
(48) Trivedi, S.; Pandey, S.; Baker, S. N.; Baker, G. A.; Pandey, S. *J. Phys. Chem. B* **2012**, *116*, 1360−1369.
(49) Fletcher, K. A.; Pandey, S. *J. Phys. Chem. B* **2003**, *107*, 13532−13539.
(50) Fletcher, K. A.; Pandey, S. *Appl. Spectrosc.* **2002**, *56*, 1498−1503.
(51) Seddon, K. R.; Stark, A.; Torres, M. *J. Pure Appl. Chem.* **2000**, *72*, 2275−2287.
(52) Wang, J. J.; Tian, Y.; Zhao, Y.; Zhou, K. L. *Green Chem.* **2003**, *5*, 618−622.
(53) Tokuda, H.; Baek, S. J.; Watanabe, M. *Electrochemistry* **2005**, *73*, 620−624.
(54) Trivedi, S.; Malek, N. I.; Behera, K.; Pandey, S. *J. Phys. Chem. B* **2010**, *114*, 8118−8125.
(55) Chang, T. M.; Dang, L. X.; Devanathan, R.; Dupuis, M. *J. Phys. Chem. A* **2010**, *114*, 12764−12774.
(56) Pramanik, R.; Rao, V. G.; Sarkar, S.; Ghatak, C.; Setua, P.; Sarkar, N. *J. Phys. Chem. B* **2011**, *115*, 2322−2330.
(57) Sarkar, S.; Pramanik, R.; Ghatak, C.; Setua, P.; Sarkar, N. *J. Phys. Chem. B* **2010**, *114*, 2779−2789.
(58) Hunger, J.; Stoppa, A.; Buchner, R.; Hefter, G. *J. Phys. Chem. B* **2008**, *112*, 12913−12919.
(59) Chakrabarty, D.; Chakraborty, A.; Seth, D.; Sarkar, N. *J. Phys. Chem. A* **2005**, *109*, 1764−1769.
(60) Sarkar, S.; Mandal, S.; Ghatak, C.; Rao, V. G.; Ghosh, S.; Sarkar, N. *J. Phys. Chem. B* **2012**, *116*, 1335−1344.
(61) Fleming, G. R.; Wolynes, P. G. *Phys. Today* **1990**, 36−43.
(62) Sivakumar, N.; Hoburg, E. A.; Waldeck, D. H. *J. Chem. Phys.* **1989**, *90*, 2305−2316.
(63) Velsko, S. P.; Waldeck, D. H.; Fleming, G. R. *J. Chem. Phys.* **1983**, *78* (10), 249.
(64) Velsko, S. P.; Fleming, G. R. *Chem. Phys.* **1982**, *65*, 59−70.
(65) Hara, K.; Akimoto, S. *J. Phys. Chem.* **1991**, *95*, 5811−5814.
(66) Aramendía, P. F.; Negri, R. M.; Román, E. S. *J. Phys. Chem.* **1994**, *98*, 3165−3173.
(67) Datta, A.; Mandal, D.; Pal, S. K.; Bhattacharyya, K. *Chem. Phys. Lett.* **1997**, *278*, 77−82.
(68) Pal, S. K.; Datta, A.; Mandal, D.; Bhattacharyya, K. *Chem. Phys. Lett.* **1998**, *288*, 793−798.
(69) Gangamallaiah, V.; Dutta, G. B. *J. Chem. Phys.* **2011**, *134* (6), 024706.
(70) Mali, K. S.; Dutt, G. B.; Mukherjee, T. *Langmuir* **2006**, *22*, 6837−6842.
(71) Mali, K. S.; Dutt, G. B.; Mukherjee, T. *J. Chem. Phys.* **2006**, *124* (6), 054904.
(72) Mali, K. S.; Dutt, G. B.; Mukherjee, T. *J. Chem. Phys.* **2008**, *128* (9), 124515.
(73) Gangamallaiah, V.; Dutta, G. B. *J. Chem. Phys.* **2011**, *135* (7), 174505.
(74) Sitzmann, E. V.; Eisenthal, K. B. *J. Phys. Chem.* **1988**, *92*, 4579−4580.
(75) Levitus, M.; Negri, R. M.; Aramendia, P. F. *J. Phys. Chem.* **1995**, *99*, 14231−14239.
(76) Ozawa, R.; Hamaguchi, H. *Chem. Lett.* **2001**, *30*, 736−737.
(77) Lakowicz, J. R. *Principles of Fluorescence Spectroscopy*; Plenum: New York, 1999; Vol. 2.
(78) Hazra, P.; Chakrabarty, D.; Sarkar, N. *Chem. Phys. Lett.* **2003**, *371*, 553−562.
(79) Das, P.; Chakrabarty, A.; Haldar, B.; Mallick, A.; Chattopadhyay, N. *J. Phys. Chem. B* **2007**, *111*, 7401−7408.
(80) Paul, B. K.; Samanta, A.; Guchhait, N. *Langmuir* **2010**, *26*, 3214−3224.
(81) Sarkar, N.; Das, N.; Das, S.; Datta, A.; Nath, D.; Bhattacharyya, K. *J. Phys. Chem.* **1995**, *99*, 17711−17714.
(82) Martins, C. T.; Sato, B. M.; El Seoud, O. A. *J. Phys. Chem. B* **2008**, *112*, 8330−8339.
(83) Masaki, T.; Nishikawa, K.; Shirota, H. *J. Phys. Chem. B* **2010**, *114*, 6323−6331.
(84) Klijn, J. E.; Engberts, J. B. F. N. *J. Am. Chem. Soc.* **2003**, *125*, 1825−1833.
(85) Reichardt, C. *Pure Appl. Chem.* **2008**, *80*, 1415−1432.
(86) Reichardt, C. *Chem. Rev.* **1994**, *94*, 2319−2358.
(87) Sarkar, D.; Bose, D.; Mahato, A.; Ghosh, D.; Chattopadhyay, N. *J. Phys. Chem. B* **2010**, *114*, 2261−2269.
(88) Waldeck, D. H. *Chem. Rev.* **1991**, *91*, 415−436.
(89) Velsko, S. P.; Fleming, G. R. *J. Chem. Phys.* **1982**, *76* (10), 3553.